

ASYMMETRIES AND ANOMALOUS PHENOMENA
IN IONIC TRANSPORT THROUGH NANOCHANNELS*I.D. KOSIŃSKA^{a,b} A. FULIŃSKI^b^aTheoretische Physik I, Institut für Physik, Universität Augsburg
Universitätsstr. 1, 86135 Augsburg, Germany^bM. Smoluchowski Institute of Physics, Jagellonian University
Reymonta 4, 30-059 Kraków, Poland*(Received October 11, 2006)*

Biological and synthetic nanochannels exhibit two essential biophysical properties: selective ion conduction and the ability to gate open in response to appropriate stimulus. Both these properties are related to several untypical modes of behaviour of the diffusional and conduction currents, absent in the normal (electro-)diffusion. We present our recent results concerning some of such anomalous phenomena. Selectivity is related to the fact that electrical and diffusive currents exhibit several asymmetries — the asymmetric channels rectify the electric currents: the relation I versus U is asymmetric (this is related to the pumping effect observed in synthetic nanochannels), moreover, for $U = 0$ the magnitude of purely diffusional currents depends on the direction of the concentration gradient. These phenomena can be described by a model based on the continuous description starting from the Smoluchowski equation. The flicker noise in the power spectra of ionic currents is known to be present both in very narrow biological and (some) synthetic channels. We simulated the motion of K^+ ions of the single-file type through a model channel with the gate which opens and closes under influence of both random noise, and interactions with ions present inside the channel. We found that there is a range of the varied parameters, in which the power spectrum has the characteristics of the flicker noise. Critical for the appearance of the flicker noise are the condition of single-file motion of ions through the channel and the opening/closing of the gate.

PACS numbers: 05.40.Ca, 87.16.Uv, 87.15.Ya, 05.10.Gg

* Presented at the XIX Marian Smoluchowski Symposium on Statistical Physics, Kraków, Poland, May 14–17, 2006.

1. Introduction

Transport of material through biological nanochannels is the basis of almost all life processes [1]. On the other hand, nanochannels transport plays an important role in biotechnology, where, for example, the nanochannels function as bio-sensors suitable for single-molecule detection [2], as well as they act as nano-pumps able to transport ions [3] or water [4] against their concentration gradients.

When the dimensions of objects approach the nanometer scale we observe new properties occurring due to the restricted geometry. Indeed, processes going in nanometer sized biological ion channels embedded in the cell membrane exhibit several untypical modes of behaviour not present in macro-scales as rectification of currents, ion selectivity, and flicker noise being present in passive channels, and pumping of material against concentration gradient, being the main function of active channels (ATPases).

Biologists tended to explain these phenomena by “specific properties” of proteins forming biological channels. However, the synthetic nanochannels which do not contain any proteins, exhibit the same peculiarities as biological passive channels including selectivity, rectification and flicker noise [5,6]; moreover, the same synthetic channels seem to be even more universal than passive biological channels, being able to pump ions against their concentration gradients [3], in which they mimic the action of active biological active channels.

The known data about these channels show that most of them is asymmetric and charged. In some, especially biological ones, the concentration gradients and/or electric charge gradients, and the motion of channel walls’ constituents are observed [6,7]. The single-file motion [8], and the values of parameters which are different from those in the bulk (macroscopic) ones [9] are expected in very narrow channels.

In this paper we present evidence that all the above-mentioned properties of nanotransport result from the confined geometry and asymmetries of very narrow channels. Most of the analysis will be devoted to ionic transport.

2. Continuous description — conductance

The description of the transport through nanosized pores by continuous models based on the Smoluchowski equation are much simpler for practical use than the more detailed microscopic ones. Although the validity of such description was subject of vivid controversy [10–15], we found recently [16–21] that the Smoluchowski equation is sufficient for at least semi-quantitative description of these rather complicated phenomena occurring on a nanoscale when the channel’s diameter is not too narrow and does not force the particles (ions) to move in a single-file arrangement. Therefore, the

model presented below will be useful mainly for the description of synthetic nanochannels in which the diameter in the narrowest part is of the order of several molecular diameters, and its applicability to biochannels is not clear.

Main physical quantities determining the model are the geometry and the electric potential inside the channel, whereas the measured quantity is the electric current through the channel. Most of the experimental [17, 18, 20] data on which the model is based were obtained in long thin channels of roughly conical geometry (*cf.* Fig. 1). The electric potential *energy* of an ion inside the channel is $\phi_i = eZ_iV$, where Z_i is ion's valence, V — the electric *potential*, e — the elementary charge. V is measured in Volts.

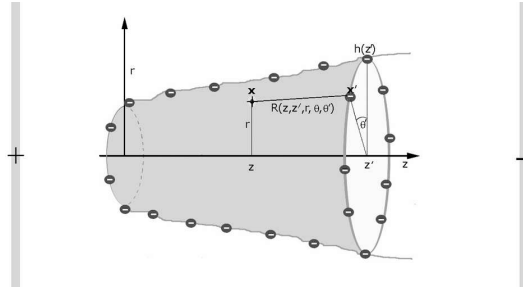


Fig. 1. Schematic sketch of the nanochannel geometry. Not in proportions.

The whole electric potential is the sum of external and internal contributions:

$$V(\mathbf{x}) \approx V_{\text{int}}(\mathbf{x}) + V_{\text{ext}}(\mathbf{x}). \quad (1)$$

The internal field is generated by the charges located on the channel walls, of charge density $es_{\text{int}}\rho(z)$, dependent in general on the location along the channel axis. We assume that the internal potential depends only on z and r (distance perpendicular to the axis) and does not depend on the angle θ (*cf.* Fig. 1 for explanation of the notation):

$$V_{\text{int}}(z, r) = \frac{es_{\text{int}}}{4\pi\epsilon} \int_0^L dz' \rho(z') h(z') \int_{-\pi}^{\pi} d\theta' R^{-1}(z, z', r, \theta') e^{-\lambda R(z, z', r, \theta')}, \quad (2)$$

where s_{int} is the sign of the walls' charge, ϵ denotes the dielectric constant (for water solutions we assume $\epsilon = 80.1\epsilon_0$, ϵ_0 being the vacuum permittivity), $\lambda = 1/l_D$ is the inverse Debye (screening) length, factor $h(z') \int_{-\pi}^{\pi} d\theta'$ gives the number of charges per unit length on the pore's circumference,

$$R(z, z', r, \theta') = |\mathbf{x} - \mathbf{x}'| = \sqrt{[r - h(z') \cos \theta']^2 + [h(z') \sin \theta']^2 + (z - z')^2}, \quad (3)$$

is the distance between points \mathbf{x} and \mathbf{x}' , and where we put $\theta = 0$, due to the assumed axial symmetry of the channel.

The mass current through the inside of the channel (bulk or volume current) can be calculated from the Smoluchowski equation in the one-dimensional Fick–Jacob’s projection [22] (*cf.* [16–19] for more details):

$$J_i = D_i \left[e^{\beta_i \bar{\phi}_i(z_0)} \bar{c}_i(z_0) - e^{\beta_i \bar{\phi}_i(z)} \bar{c}_i(z) \right] / \int_{z_0}^L dz' A^{-1}(z') e^{\beta_i \bar{\phi}_i(z')}. \quad (4)$$

and the corresponding concentration profile reads:

$$e^{\beta_i \bar{\phi}_i(z)} \bar{c}_i(z) = e^{\beta_i \bar{\phi}_i(z_0)} \bar{c}_i(z_0) - \frac{J_i}{D_i} \int_{z_0}^z dz' A^{-1}(z') e^{e Z_i \beta \bar{\phi}_{i,\text{int}}(z')}, \quad (5)$$

where $\bar{c}_i(z)$ and $\bar{\phi}_i(z) = e Z_i \bar{V}(z)$ are the concentration and electric potential energy of the ion i averaged over the channel’s cross-section $A(z) = \pi h^2(z)$, and $\beta = 1/kT$.

The standard procedure (*cf.* *e.g.* [23]) is to calculate V_{int} , \bar{V}_{int} , and J_i from the assumed zeroth approximation for the concentration gradient $\bar{c}(z, r)$ (*e.g.* bulk value $c(z) = c_0 + (c_L - c_0)z/L$), next to calculate $\bar{c}_i(z, r)$ from the above functions: $\bar{c}_i(z, r) = \bar{c}_i(z)$; $\bar{V}_{\text{int}}(z, J_i) = \exp[-\beta e Z_i V_{\text{int}}(z, r)]$, and so on.

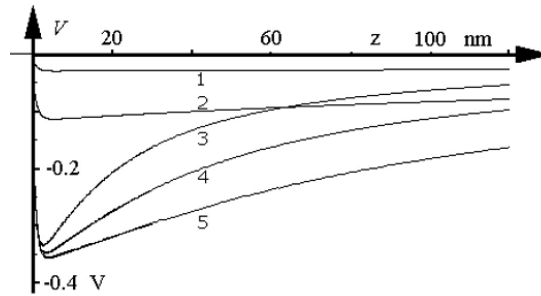


Fig. 2. The shape of the effective electric potential inside the nanochannel resulting from the uniform charge distribution on the surface of the conical pores of different sizes. External field is not taken into account. $L = 12 \mu\text{m}$, constant surface charge $\rho = 1.5e/\text{nm}^2$ and concentrations on both sides 0.1 M. Curve 1: $r_0 = 1 \text{ nm}$, $r_L = 1000 \text{ nm}$, curve 2: $r_0 = 1 \text{ nm}$, $r_L = 500 \text{ nm}$, curve 3: $r_0 = 20 \text{ nm}$, $r_L = 250 \text{ nm}$, curve 4: $r_0 = 5 \text{ nm}$, $r_L = 250 \text{ nm}$, curve 5: $r_0 = 1 \text{ nm}$, $r_L = 250 \text{ nm}$. The potential near pores’ wide aperture is of the order of 10^{-4} V .

The typical shapes of the effective potential $\bar{V}(z)$ and of the concentration profiles are shown in Figs. 2 and 3. The important feature is the asymmetric minimum of the potential near the narrow tip of the conical pore, which is the main source of the selectivity, rectification, and pumping by charged nanochannels (*cf.* below).

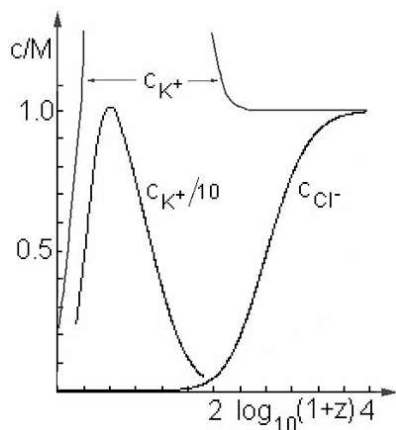


Fig. 3. Concentration profiles of cations (K^+) and anions (Cl^-) inside the conical nanopore of dimensions $r_0 = 1.5 \text{ nm}$, $r_L = 315 \text{ nm}$, $L = 12 \mu\text{m}$, constant surface charge $\rho = 1.5e/\text{nm}^2$ and concentration gradient: $c_0 = 0.1$, $c_L = 1.0 \text{ M}$ KCl. Note the logarithmic scale.

The bulk electric current $I_b = e \sum_i t_i Z_i J_i$, where t_i are the so-called transference numbers of cations (t_+) and anions (t_-) (for bulk KCl $t_+ \approx t_- \approx 0.5$) is not the sole contribution to the measured current. As a result of strong interactions between the charges on the pore walls and the ions in the solution, there is a surface (called also double or diffuse) layer [23, 24], formed close to the pore walls. The surface layer contains mainly counterions to the charges on the pore walls. The counterions move along the applied field and contribute to I . Both literature [23, 24] and our experimental data [17, 18] show that this effect is especially strong in very narrow pores, and at lower concentrations when the double-layer thickness becomes larger. Therefore,

$$I = I_b + I_s. \quad (6)$$

Evidence of the surface currents (in the form of the concentration dependence of the conductivity $\kappa(c)$) is shown in Fig. 4 for a cylindrical synthetic nanochannel [17] without any asymmetry which could be responsible for the observed effect. The data and curves labelled “pH 8” and “pH 2” correspond to negatively charged and electrically neutral, respectively, channels (*cf.* [17] for more details), the curve “bulk” presents the conductivity calculated in

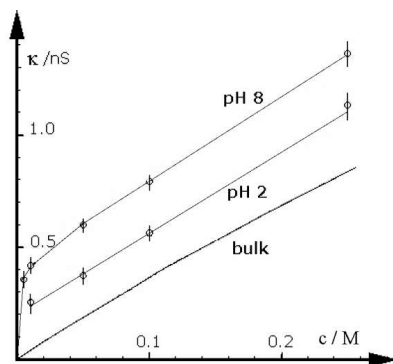


Fig. 4. Determination of the surface conductance κ versus concentration c of the solutions of KCl κ in the cylindrical nanochannel, $L = 12 \mu\text{m}$, $r_0 = r_L = 35 \text{ nm}$. Circles: experimental data with experimental error shown by vertical bars.

the absence of surface currents. The difference between conductivities of charged and neutral channels is interpreted as the surface conductivity. Note the strong nonlinearity of the conductance in the charged pore as function of concentration at low concentrations of KCl, being the effect of changes of parameters, mainly ionic mobilities and Debye screening lengths, in the strongly confined geometries [9].

The ionic selectivity results from the concentration profiles inside asymmetric nanochannels shown in Fig. 3, the cations are attracted towards, anions, repelled from the narrow opening. The calculated cationic and anionic diffusional flows J through short narrow nanopore of dimensions comparable to biological channels are shown in Fig. 5. The positive direction of flow (along concentration gradient and external electric field) is from narrow to wide opening.

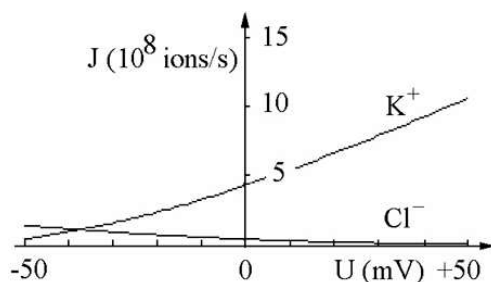


Fig. 5. Asymmetry of ionic nanocurrents: electro-diffusional flows of K^+ and Cl^- through short narrow nanochannel of dimensions $r_0 = 0.5 \text{ nm}$, $r_L = 1.5 \text{ nm}$, $L = 6 \text{ nm}$, constant surface charge $\rho = 1.6e/\text{nm}^2$ and concentration gradient $c_0 = 1.0$, $c_L = 0.1 \text{ M}$ KCl.

Both the model and electrolytic conductivity measurements show that asymmetric nanopores rectify partially the current, even in relatively wide channels. This is illustrated Fig. 6. The preferential direction of cation flow is from the high towards the low surface charge density and/or from the narrow towards the wide opening of the pore, *i.e.* from high towards low electric fields.

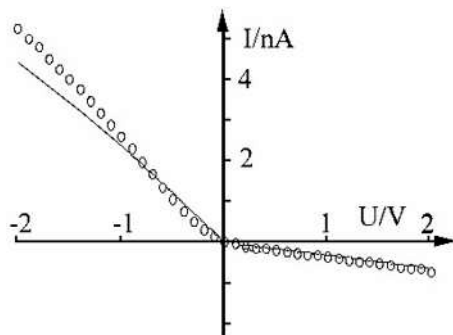


Fig. 6. Rectification of ionic nanocurrents: current-voltage characteristic of a single conical synthetic pore of dimensions $r_0 = 12$ nm, $r_L = 710$ nm, $L = 12$ μ m, constant surface charge $\rho = 1.5e/\text{nm}^2$ and constant concentration $c_0 = c_L = 0.1$ M KCl. Circles: experimental data [18], continuous line: fitted model.

When the driving (external) field is oscillating, the rectification effect results in the pumping of ions against concentration gradient. This type of pumping, shown in Fig. 7, is observed experimentally in synthetic nanopores [3]. Biological pumps (ATPases) work by different principle, using the energy from the dissociation of ATP, although they are also able to make use of the energy from the oscillating electric field [25]. Common factor for both

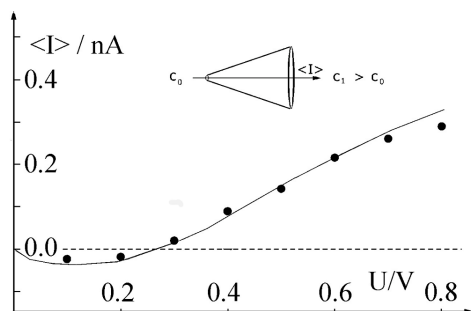


Fig. 7. Pumping of ions against concentration gradient by periodic electric field through synthetic conical pore of dimensions $r_0 = 1.5$ nm, $r_L = 315$ nm, $L = 12$ μ m, constant surface charge $\rho = 1.5e/\text{nm}^2$ and concentration gradient: $c_0 = 0.1$, $c_L = 1.0$ M KCl. Circles: experimental data [3], continuous line: model with fitted parameters [3] (*cf.* also [14]).

types of nanopumps is that they work by the so-called ratchet principle, *i.e.* due to asymmetry of electric potentials [3, 26, 27]. It was shown that the pumping by ATPases is related to the stochastic resonance [26].

Still other, unknown earlier effect is shown in Fig. 8. When the concentration gradient through asymmetric nanopore is reversed, not only the direction of the (electro-)diffusional flow J is reversed, but also changes its magnitude [19–21], with the preferential direction (higher $|J|$) from the wide towards the narrow opening. Fig. 8 shows also the difference between flows calculated according to the bulk (dashed lines) and fitted (continuous lines) values of the model physical parameters. Although the bulk-type version of the model does not describe the experimental data too well, it still gives qualitatively correct predictions of the asymmetry effects.

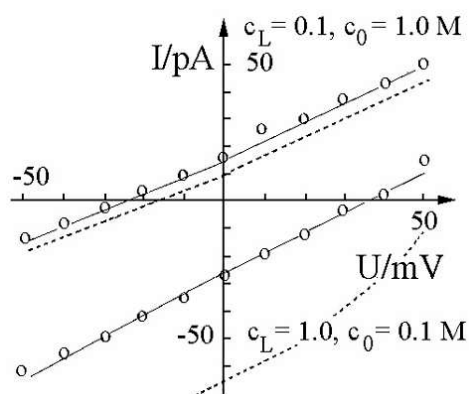


Fig. 8. Asymmetry of the nanodiffusion: ionic currents through synthetic conical pore of dimensions $r_0 = 1.5$ nm, $r_L = 315$ nm, $L = 12$ μ m, constant surface charge $\rho = 1.5e/\text{nm}^2$ and concentration gradient: $c_0 = 0.1$, $c_L = 1.0$ M KCl. Circles: experimental data [19, 20], continuous line: model with fitted parameters, dashed line: model with bulk parameters.

3. Brownian Dynamics — flicker noise

Ion currents through nanochannels exhibit fluctuations of the type of $1/f$ (flicker) noise when a constant voltage is applied. Moreover, the power spectra of the currents through biological and synthetic channels are almost identical (*cf.* Fig. 9), originate from the channel’s opening–closing processes and most probably are related to the motion of charged constituents of the pore walls [6]. These facts are related to the hypothesis put forward earlier in [7] that this type of noise is produced by “fluctuator” dynamics, that is, by random switching of the channel between its different conducting states. Such, well-known, switching of channel-forming proteins between their conformations is called “gating”.

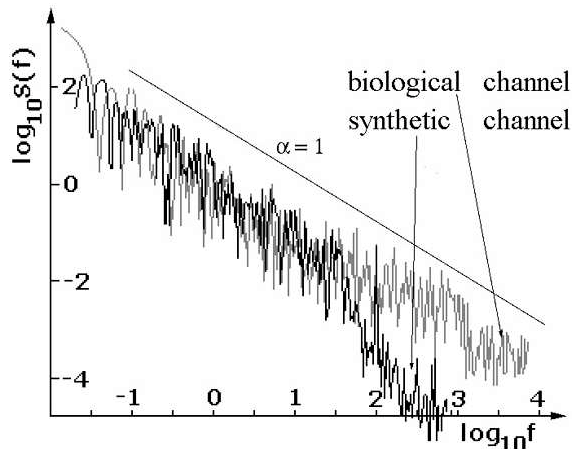


Fig. 9. Comparison of experimental power spectra of K^+ currents through biological and synthetic nanochannels (*cf.* [6] for details).

In very narrow pores of dimensions in the narrow part comparable with biological channels the ions (or other particles) can move in a single-file formation only. In such a case the molecular dynamics (MD) simulations seem to be more reliable than the continuous-type description via (electro-) diffusional equations, discussed in the preceding section.

MD simulations of molecular structure of biological or synthetic K^+ channels containing ions and water inside and in the immediate vicinity, *etc.*, requires use of total number of atoms in the simulation system above 4×10^4 , and time-steps 0.2 fs [28,29]. Therefore, we chose the semi-heuristic approach, keeping correct equations of motion (in the form of Langevin-type equations) and correct interactions between ions, but substituting the random and friction forces for the interactions with water molecules, and introducing more or less heuristic assumptions about interactions of ions with the channel walls. For this latter purpose the following known properties of the ionic transport through narrow channels were used: *(i)* single-file motion, *(ii)* gating — it was shown that in synthetic channel it results from the motion of so-called “dangling ends”, *i.e.* of the cleaved charged polymer strands [6], whereas in biological channels several more or less plausible gating mechanisms were proposed, including conventional mechanical ideas of swinging door or slider obstructing the pore [1], *(iii)* asymmetry of the shape and of internal potential (in synthetic channels $V_{\min}(z)$ lies at about 5 nm from the narrow tip, *cf.* Fig. 2), *(iv)* concentrations outside channel different in biological cells, the same in synthetic channel measurements [6], *(v)* length of biological channels about 10 nm, synthetic channels are much longer, with the narrow part (tip) a few nm long.

These features were modelled by: *(i)* quasi-one-dimensional motion plus “no jump” condition, *(ii)* charged gate inside channel, *(iii)* external charges pushing cations towards centre of pore, simulating the asymmetric forces from charged channel’s walls acting on ions (*cf.* Figs. 2 and 3 above), *(iv)* the assumption that cations enter the pore (simulation region) with probabilities $P_{\text{in},0}$, $P_{\text{in},L}$ (the same or different), *(v)* simulation region of length $L = 10$ nm. Moreover, we used two different types of the description of the opening and closing of the gate: *(i)* the Langevin-type equations of motion for charged dangling ends treated as two-dimensional pendula interacting with each other and with passing ions [30], and *(ii)* the heuristic gate which opens and closes depending whether the force acting on it is higher or lower than some prescribed value (*cf.* below, Eq. (9) [31, 32]).

Contrary to noiseless Molecular Dynamics, the selection of the time-step δt cannot be done at will, but it needs to meet some additional conditions [12, 32, 33], which result in the requirement that δt to be of the order of m/γ , m being the ion’s mass, γ — the friction coefficient. In our simulations, for K^+ ions in water, this gives $\delta t \approx 31$ fs.

All the above assumptions lead to the following equations describing our Brownian Dynamics model:

the Langevin-type equations of motion for the cations moving along the z -axis of the channel:

$$\begin{aligned} m_i \dot{v}_i &= -\gamma_i v_i + R_i(z_i) + F_i(z_i), \\ \dot{z}_i &= v_i, \end{aligned} \quad (7)$$

where v_i is the velocity of i -th ion, z_i — the position, m_i — the mass, γ_i — the friction coefficient, and either analogous equations for dangling ends’ gate:

$$I \dot{\vec{\omega}}_k = -\tilde{\gamma}_k l_k^2 \vec{\omega}_k + \vec{l}_k \times \vec{R}_k + \vec{l}_k \times \vec{F}_{gk}, \quad (8)$$

where m_i is the mass of i -th ion, γ_i — the friction coefficient, $\vec{\omega}_k$, I_k and l_k — angular velocity, inertia and length of the k -th dangling end, or the expression for the total force acting on the heuristic gate:

$$F_{\text{tot},g} = F_g + Q_g R_g. \quad (9)$$

Here F_i , F_g are sums of deterministic forces, R_i , R_k — the random forces assumed here to be the thermal noise represented by the Gaussian white noise, and R_g — the Wiener process (gate’s Brownian motion). Friction coefficients are assumed to result from the water viscosity η via the Stokes law.

The deterministic forces experienced by an i -th cation, k -th dangling end, and the gate consist of (i) the applied external force (U — the electrical potential difference between two symmetrically (far away from the channel) located points, L — length of the channel):

$$F_{\text{ext},j} = -q_j(U/L)\hat{z}, \quad j = i, g, \tag{10}$$

(ii) the standard internal Coulomb force between all the charges q_j (cations and dangling ends or gate’s charge), and (iii) the short-range repulsive forces between ions [12, 34]:

$$F_{\text{SR},i} = \sum_{m \neq i} F_{\text{SR},im} = F_{\text{SR}} \sum_{m \neq i} \left| \frac{d_c}{z_{im}} \right|^{11} \frac{z_{im}}{d_c}, \tag{11}$$

where the sum over m runs over all the ions in the system, with additional condition that ions cannot pass through closed gate. $z_{im} = z_i - z_m$, d_c is the nearest approach distance between two ions (“soft-sphere” diameter).

The simulations of the above equations were performed with the “forward evaluation” (cf. [31, 32, 34]):

$$\begin{aligned} m_i \frac{v_{i,n+1} - v_{i,n}}{\delta t} &= -\frac{1}{2} \gamma_i(v_{i,n} + v_{i,n+1}) + R_{i,n} + F(\{z_{i,n}\}), \\ \frac{z_{i,n+1} - z_{i,n}}{\delta t} &= v_{i,n+1}. \end{aligned} \tag{12}$$

Non-standard part is the simulation of single-file motion [32]. Description of the details of that procedure are given in the Appendix, and the code can be found in Archives [31].

We used in the simulations the values of parameters corresponding to potassium cations K^+ with atomic mass $M_{\text{K}^+} = 39 \text{ u}$ ($= 6.5 \times 10^{-26} \text{ kg}$), radius $r_{\text{K}^+} = 0.133 \text{ nm}$, and charge $+e$ ($Z_{\text{K}^+} = 1$). The initial velocities of the particles were chosen from the Maxwell distribution with room temperature. The physical parameters were kept constant, varied were values of the external and heuristic parameters such as voltage U , “concentrations” (entrance probabilities P_{in}) outside the simulation region, height of the gate’s barriers, etc.

Simulations provided the series of values of net numbers m of cations passing through the channel in one simulation step δt , i.e., the momentary ionic currents. From these series the frequency spectra were calculated in a standard way. In all simulations first 10^6 steps were rejected, and the power spectra were calculated from runs of length 0.5 to $1 \times 10^7 \delta t$. We found that there is a narrow range of the varied parameters, in which the power spectrum has the characteristics of the flicker noise, independent whether we

use the heuristic gate, or the motion of dangling ends. This result is shown in Fig. 10. The flicker-noise character is clearly visible: $S(f) \sim f^{-\alpha}$, with $\alpha = 1.05 \pm 0.1$.

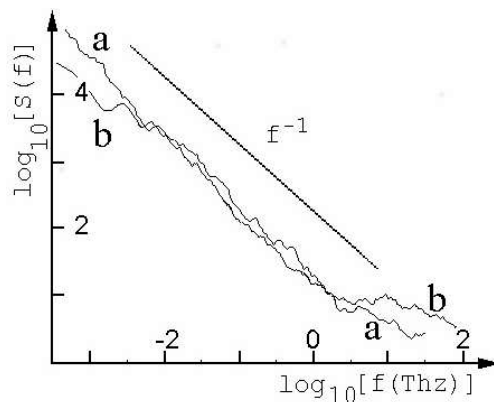


Fig. 10. Power spectra of K^+ current calculated from the Brownian Dynamics model with two different gating mechanisms: (a) “dangling ends”, (b) heuristic gate (*cf.* text).

Calculations with various sets of model parameters revealed that crucial for the appearance of the flicker noise in the ionic nanocurrents are the gating process itself and the single-file motion. When these conditions are relaxed, the power spectra behave as $f^{-1.5}$ or f^{-2} .

4. Final remarks and conclusions

Continuous-type description (modelling) of the ionic transport through synthetic nanopores, discussed in Section 2, seems to work surprisingly well when one allows for the non-bulk values of some physical parameters characterising the electrolyte solutions, mainly the mobilities and Debye screening. On the other hand, the use of bulk values of these parameters still gives qualitatively correct predictions of the asymmetry effects and, therefore, can be used for the rough predictions in the construction of nanopores of desired properties. It is worth noticing in this context that rectification, asymmetrical diffusion, and cation/anion selectivity are present in relatively wide nanopores of diameters in the narrow parts of the order of magnitude wider than several particle diameters.

The continuous model not only reproduces correctly the known nanoeffects: cation/anion selectivity, rectification and pumping, it also helped in establishing new features such as the contribution of surface cationic currents, and the discovery of the asymmetry of nanodiffusion. Moreover, the model — together with other independent calculations of the continuous

character [21] — showed that all these nanoeffects derive solely from the asymmetries of the confined geometrical conditions and of the electrical fields inside nanochannels and that, therefore, “specific properties” of proteins are unimportant. However, there remains the open question whether specific properties of proteins are necessary for cation/cation selectivity?

The continuous model predicts all mentioned above peculiarities of the nanotransport, except the appearance of the flicker noise. The latter can be modelled by the Brownian Dynamics (Section 3 above). It was found that critical for the appearance of the flicker noise are the condition of single-file motion of ions through the channel and the opening/closing of the gate.

The results presented in Section 3 show also that, although the gating process itself is crucial for the appearance of the flicker noise in the ionic nanocurrents, the details of the gating mechanism are unimportant from this point of view.

It is worth to note that the flicker noise in nanochannels is accompanied by the non-Markovian character of the current treated as the stochastic time-series [6, 30, 35].

The essential message from the works presented in this paper is that all the anomalous phenomena characteristic of ionic nanotransport result from the confined geometry and from asymmetries of electric fields inside nanochannels.

Appendix A

Here we present the description of the procedures for the single-file motion. The procedures for entrances and exits of particles, for the number of particles located to the left of the gate, as well as the codes for the determination of the state of the gate (open or closed), and for the equations of motion are standard and will not be discussed here.

Single-file procedures are based on the fact that the given particle (cation) i cannot move farther than its neighbours $i - 1$ and $i + 1$, which in turn are limited by their neighbours, i and $i - 2$ or $i + 2$, *etc.* Therefore, their positions need to be recalculated. In the simplest version, it is assumed that particles meet at the middle of their former positions. In better versions such a pair of particles meets at the position calculated from their former positions and from their new velocities. On the other hand, the particles retain their velocities until a given pair meets, then they collide and — in the simplest version — exchange their velocities (behave as hard spheres). Again, it is possible to refine this simplest procedure. Because the results of the above-described procedure depend on whether the recalculations are done “up” or “down”, *i.e.*, from particle number 1 to N , or from N to 1, both reordering need to be realized independently, their results averaged, and the whole scheme iterated until self-consistency is attained.

REFERENCES

- [1] B. Hille, *Ionic Channels of Excitable Membranes*, Sinauer, Sunderland, MA 1992 (2-nd Edition).
- [2] See e.g. S.M. Bezrukov, I. Vodyanoy, V.A. Parsegian, *Nature* **370**, 279 (1994); J.J. Kasianowicz, E. Brandin, D. Branton, D.W. Deamer, *Proc. Natl. Acad. Sci. USA* **93**, 13770 (1996); A. Mara, Z. Siwy, Ch. Trautmann, F. Kamme, *Nano Letters* **4**, 497 (2004) and references therein.
- [3] Z. Siwy, A. Fuliński, *Phys. Rev. Lett.* **89**, 198103 (2002); *Am. J. Phys.* **72**, 567 (2004).
- [4] O. Hod, E. Rabani, *PNAS* **100**, 14661 (2003).
- [5] C.A. Pasternak, C.L. Bashford, Y.E. Korchev, T.K. Rostovtseva, A.A. Lev, *Coll. Surf.* **A77**, 119 (1993); Y.E. Korchev, C.L. Bashford, G.M. Alder, P.Y. Apel, D.T. Edmonds, A.A. Lev, K. Nandi, E. Spohr, A.V. Zima, C.A. Pasternak, *FASEB J.* **11**, 600 (1997); Z. Siwy, Y. Gu, H. Spohr, D. Baur, A. Wolf-Reber, R. Spohr, P. Apel, Y.E. Korchev, *Europhys. Lett.* **60**, 349 (2002); Z. Siwy, D.D. Dobrev, R. Neumann, C. Trautmann, K. Voss, *Appl. Phys.* **A76**, 781 (2003).
- [6] Z. Siwy, A. Fuliński, *Phys. Rev. Lett.* **89**, 158101, (2002); in *Unsolved Problems of Noise and Fluctuations*, Proc. Third Int. Conf. UPoN, Washington 2002, Ed. by S.M. Bezrukov, World Scientific, Singapore 2003, pp. 273–282.
- [7] S.M. Bezrukov, M. Winterhalter, *Phys. Rev. Lett.* **85**, 202 (2000).
- [8] Cf. e.g. B. Hille, W. Schwarz, *J. Gen. Physiol.* **72**, 409 (1978); S. Berneche, B. Roux, *Nature* **414**, 73 (2001); K.K. Mon, J.K. Percus, *J. Chem. Phys.* **117**, 2289 (2003) and references therein.
- [9] W. Im, B. Roux, *J. Mol. Biol.* **319**, 1177 (2002); A. Alcaraz, E.M. Nestorovich, M. Aguilera-Arzo, V.M. Aguilera, S.M. Bezrukov, *Biophys. J.* **87**, 943 (2004); Y-C. Liu, Q. Wang, L-H. Liu, *J. Chem. Phys.* **120**, 10278 (2004).
- [10] J.A. Quinn, J.L. Anderson, W.S. Ho, W.J. Petzny, *Biophys. J.* **12**, 990 (1972); M. Glasser, *Phys. Lett.* **A300**, 381 (2002); J.B. Freund, *J. Chem. Phys.* **116**, 2194 (2002).
- [11] W. Nonner, D.P. Chen, B. Eisenberg, *J. Gen. Physiol.* **113**, 773 (1999); D.G. Levitt, *J. Gen. Physiol.* **113**, 789 (1999).
- [12] G. Moy, B. Corry, S. Kuyucak, S.H. Chung, *Biophys. J.* **78**, 2349 (2000); B. Corry, S. Kuyucak, S.H. Chung, *Biophys. J.* **78**, 2364 (2000).
- [13] D. Woermann, *Nucl. Instrum. Methods Phys. Res.* **B194**, 458 (2002); *Phys. Chem. Chem. Phys.* **5**, 1853 (2003); P. Ramirez, S. Mafé, V.M. Aguilera, A. Alcaraz, *Phys. Rev.* **E68**, 011910 (2003).
- [14] C. Rischel, H. Flyvbjerg, *Phys. Rev. Lett.* **91**, 179801 (2003).
- [15] Z. Siwy, A. Fuliński, *Phys. Rev. Lett.* **91**, 179802 (2003).
- [16] I.D. Kosińska, Ph.D. Thesis, Kraków 2004.
- [17] A. Fuliński, I.D. Kosińska, Z. Siwy, *Europhys. Lett.* **67**, 683 (2004).
- [18] A. Fuliński, I.D. Kosińska, Z. Siwy, *New J. Phys.* **7** 132 (2005).

- [19] I.D. Kosińska, A. Fuliński, *Phys. Rev.* **E72**, 011201 (2005).
- [20] Z. Siwy, I.D. Kosińska, A. Fuliński, C.R. Martin, *Phys. Rev. Lett.* **94**, 048102 (2005).
- [21] I.D. Kosińska, *J. Chem. Phys.* **124**, 244707 (2006).
- [22] R. Zwanzig, *J. Phys. Chem.* **96**, 3926 (1992); D. Reguera, J.M. Rubi, *Phys. Rev.* **E64**, 061106 (2001).
- [23] D. Ericson, D. Li, *J. Coll. Interface Sci.* **237**, 283 (2001); Dongqing Li, *Encyclopedia of Surface and Colloid Science*, 2002, pp. 3167–3177.
- [24] J. Israelachvili, *Intermolecular and Surface Forces*, Academlib, New York 1992.
- [25] D.-S. Liu, R.D. Astumian, T.Y. Tsong, *J. Biol. Chem.* **265**, 7260 (1990).
- [26] A. Fuliński, *Phys. Rev. Lett.* **79**, 4926 (1997); *CHAOS* **8**, 549 (1998).
- [27] R.D. Astumian, I. Derenyi, *Eur. Biophys. J.* **27**, 474 (1998).
- [28] S. Berneche, B. Roux, *Nature* **414**, 73 (2001).
- [29] J.N. Sachs, P.S. Crozier, T.B. Woolf, *J. Chem. Phys.* **121**, 10847 (2004).
- [30] I.D. Kosińska, A. Fuliński, *Background Processes and the Generation of the Flicker Noise in Nanochannel Transport*, in *Unsolved Problems of Noise and Fluctuations: UPoN 2005*, Ed. by L. Reggiani, C. Pennetta, V. Akimov, M. Rosini, AIP CP800 (2005), pp. 287–292.
- [31] I.D. Kosińska, A. Fuliński, [physics/0603238](#)
- [32] I.D. Kosińska, A. Fuliński, *Acta Phys. Pol. B* **37**, 1745 (2006).
- [33] A. Singer, Z. Schuss, *Phys. Rev.* **E71**, 026115 (2005); A. Singer, Z. Schuss, B. Nadler, R.S. Eisenberg, *Phys. Rev.* **E70**, 061106 (2004).
- [34] S. Kuyucak, O.S. Andersen, S-H. Chung, *Rep. Prog. Phys.* **64**, 1427 (2001).
- [35] A. Fuliński, Z. Grzywna, I. Mellor, Z. Siwy, P.N.R. Usherwood, *Phys. Rev.* **E58**, 919 (1998); Z. Grzywna, Z. Siwy, A. Fuliński, I. Mellor, P.N.R. Usherwood, *Cell. Mol. Biol. Lett.* **4**, 37 (1999).